M&C 2017 - International Conference on Mathematics & Computational Methods Applied to Nuclear Science & Engineering, Jeju, Korea, April 16-20, 2017, on USB (2017)

Progress of Cumulative Migration Method for Computing Diffusion Coefficients with OpenMC

Zhaoyuan Liu, Kord Smith, Benoit Forget

Nuclear Science & Engineering Department, Massachusetts Institute of Technology
77 Massachusetts Ave, Cambridge, MA, USA
liuzy@mit.edu, kord@mit.edu, bforget@mit.edu

Abstract - *The cumulative migration method (CMM) is a new method for computing diffusion coefficients and transport cross sections in light water reactors that is both rigorous and computationally efficient. It eliminates the sources of inaccuracy in the commonly applied "out-scatter" transport correction. The newly developed method is directly applicable to lattice calculations performed by Monte Carlo and is capable of computing rigorous homogenized diffusion coefficients for arbitrarily heterogeneous lattices. Directional diffusion coefficients can also be computed in a natural approach using CMM. In this paper the group-wise tally scheme for CMM is introduced. The group-wise tally is functionally equivalent to cumulative-group tally but allows for simple integration into existing Monte Carlo codes.*

I. INTRODUCTION

In the calculation of multi-group diffusion coefficients and transport cross sections, the "out-scatter" approximation is a widely adopted approach in production lattice physics codes [1, 2, 3, 4]. It assumes that the in-scatter rate of neutrons from energies E' to E will approximately balance the out-scatter rate of neutrons from E to all other energies. The approximation can be represented as

$$\int_0^\infty \Sigma_{s1}(\boldsymbol{r}, E' \rightarrow E)\boldsymbol{J}(\boldsymbol{r}, E')dE' \approx \int_0^\infty \Sigma_{s1}(\boldsymbol{r}, E \rightarrow E')\boldsymbol{J}(\boldsymbol{r}, E)dE' \tag{1}$$

in which $\Sigma_{s1}(\boldsymbol{r}, E' \rightarrow E)$ is the P_1 scattering cross section from E' to E at position $\boldsymbol{r}$, and $\boldsymbol{J}(\boldsymbol{r}, E')$ is the neutron current at energy E' and position $\boldsymbol{r}$. Based on this approximation, the multi-group transport cross section is expressed as given in Equation (2a), in which $\Sigma^{os}_{tr,g}$ is the transport cross section from the out-scatter approximation, $\Sigma_{t,g}$ is the total cross section, $\Sigma_{s0,g}$ is the P_0 scattering cross section, $\overline{\mu}_g$ is the average scattering cosine, and subscript g denotes the group index. The spatial dependence on $\boldsymbol{r}$ is omitted in subsequent equations for a clearer expression.

Since elastic scattering with ^{1}H can be seen as purely isotropic in the center-of-mass system, $\overline{\mu}_g$ can be shown to be $2/3$ when thermal scattering effects are neglected. This induced an easier way of computing diffusion coefficients by taking $\overline{\mu}_g$ to be $2/3$ for all groups, with $\Sigma^{as}_{tr,g}$ defined as the transport cross section from the "asymptotic" out-scatter approximation.

Another method makes the hypothesis that neutron current can not exceed the scalar flux and it uses scalar flux spectrum instead of neutron current spectrum for weighting the P_1 scattering cross sections [5]. The transport cross section computed by this method as shown in Equation (2b) can be called the "flux-limited" transport cross section. In Equation (2b) ϕ_g is scalar flux in group g and $\Sigma_{s1,g'\rightarrow g}$ is the P_1 cross section of scattering from group g' to group g.

$$\Sigma^{os}_{tr,g} = \Sigma_{t,g} - \overline{\mu}_g\Sigma_{s0,g} \tag{2a}$$

$$\Sigma^{fl}_{tr,g} = \Sigma_{t,g} - \sum_{g'=1}^{G}\frac{\Sigma_{s1,g'\rightarrow g}\phi_{g'}}{\phi_g} \tag{2b}$$

The deficiency of these approximations has been shown in a previous paper [6] using a simple model with pure hydrogen uniformly distributed in infinite medium. The results from the three approximation methods are compared with those computed from solving P_1 equations and show deviations of roughly 30% in the fast group.

The Cumulative Migration Method (CMM) for computing homogenized assembly multi-group diffusion coefficients and transport cross sections is both rigorous and computationally efficient [6]. In the limit of a homogeneous hydrogen slab, this method is equivalent to the long-used CASMO transport method [7]. The new method can be directly tallied in Monte Carlo methods and provides better accuracy than the previously used "out-scatter" approximation. CMM is implemented in a test version of OpenMC [8], and applications of CMM to the BEAVRS benchmark problem [9] have shown significant improvement in generating accurate homogenized assembly diffusion coefficients for full-core diffusion calculations [10].

In conventional nodal diffusion calculations, material properties are generally assumed isotropic and diffusion coefficients have no variation in different directions. However, the isotropy in practical problems is never rigorously true and sometimes it can be a very poor assumption, such as in the TREAT (TRansient REactor Test facility) at the Idaho National Laboratory (INL) [11].

The TREAT fuel assemblies were designed with vertical streaming channels, which makes directional variations important axially as shown in Figure 1. Recent work on CMM demonstrates the natural extension for computing directional diffusion coefficients in Monte Carlo. An 11-group diffusion test problem of a simplified model of TREAT fuel assembly showed that both eigenvalue and flux distribution are more accurate using the directional diffusion coefficients computed by CMM.

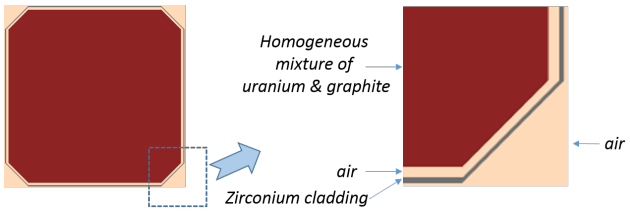

Fig. 1. The 2D geometrical layout and material composition of active fuel zone of TREAT fuel assembly.

Additionally, a new equivalent group-wise tally method has now been developed, which provides greater efficiency and is simpler to implement in conventional Monte Carlo tallies. The new tally method provides a promising bridge for computing heterogeneous diffusion coefficients and transport cross sections.

II. THEORY OF CMM

1. Migration Area

In one-group diffusion theory, the relationship between migration area M^2, diffusion coefficient D, absorption cross section Σ_a and the mean square crow flight distance of the neutrons $\langle r^2 \rangle$ is $M^2 = D/\Sigma_a = \langle r^2 \rangle/6$. Similar analysis can be done from birth to a lower energy bound. In other words, the "partial" migration area while the neutron slows down can be defined as

$$M^2(E > E_g) = \frac{D(E > E_g)}{\Sigma_r(E > E_g)} \tag{3}$$

In Equation (3), $M^2(E > E_g)$ is the cumulative migration area before the neutron's energy becomes less than E_g, $D(E > E_g)$ is the diffusion coefficient for the energy range of $[E_g, E_{max}]$, and $\Sigma_r(E > E_g)$ is the removal cross section for the energy range of $[E_g, E_{max}]$, which will include not only absorption, but also net down scatter to an energy lower than E_g.

From the perspective of energy groups, the energy range of $[E_g, E_{max}]$ can be seen as a "broad" group whose upper boundary always starts from E_{max}. In a multi-group structure, as E_g is the lower boundary of group g, then the "broad" group can be seen as a "cumulative group" from group 1 to group g. The concept of cumulative group is illustrated in Figure 2, in which the group structure is represented in the pyramid frame with cumulative group g and cumulative group $(g + 1)$ shown in shadowed areas. Based on this concept, Equation (3) can be expressed in the form of cumulative group as

$$(M_g^c)^2 = \frac{D_g^c}{\Sigma_{r,g}^c} \tag{4}$$

where the superscript c indicates that all the quantities in this equation are for the cumulative group g, that is to say, the combined "broad" group from group 1 to group g.

Equation (4) provides a scheme for computing cumulative multi-group diffusion coefficients through the theory of cumulative migration area, using the one-sixth relationship

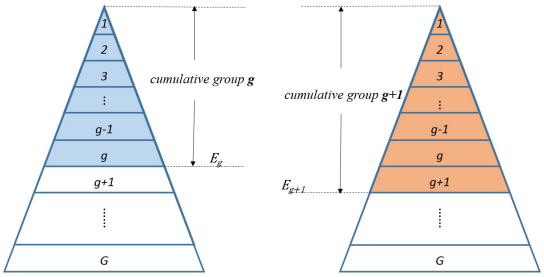

Fig. 2. Illustration of the concept of "cumulative group". (Left: cumulative group g, right: cumulative group $(g + 1)$.)

with the mean square of neutron's crow flight length, as shown as

$$(M_g^c)^2 = \frac{1}{6}\langle (r_g)^2 \rangle \tag{5}$$

where r_g is the crow flight length from the neutron's birth position to the position where it is removed from the cumulative group g, and r_g is a quantity that can be tallied directly in Monte Carlo codes. Then group-wise diffusion coefficients D_g can be calculated by "unfolding" cumulative multi-group diffusion coefficients D_g^c using flux-weighting as shown in Equation (6).

$$D_g^c = \frac{\sum_{g'=1}^{g} D_{g'}\phi_{g'}}{\sum_{g'=1}^{g} \phi_{g'}} \tag{6}$$

2. Directional Diffusion Coefficients Generation

In CMM, directional dependency can be handled naturally by projection of neutrons' cumulative migration vector to respective axes. In a Cartesian coordinate system, every track vector of the neutron's flights can be decomposed into different components by projecting according to the x, y, z axes. As shown in Figure 3, $\boldsymbol{r}$ is the neutron's cumulative migration vector, and $\boldsymbol{r}_z$ is the vertical component of $\boldsymbol{r}$. Since $\boldsymbol{r} = \boldsymbol{r}_x + \boldsymbol{r}_y + \boldsymbol{r}_z$ and $\langle (\boldsymbol{r})^2 \rangle = \langle (\boldsymbol{r}_x)^2 \rangle + \langle (\boldsymbol{r}_y)^2 \rangle + \langle (\boldsymbol{r}_z)^2 \rangle$, in isotropic materials, it is obvious that $\langle (\boldsymbol{r})^2 \rangle = 3 \cdot \langle (\boldsymbol{r}_z)^2 \rangle$. The directional diffusion coefficients can be computed by using $\boldsymbol{r}_z$ as shown in Equation (7).

$$(M_{z,g}^c)^2 = \frac{1}{6}\langle (r_{z,g})^2 \rangle \tag{7a}$$

$$D_{z,g}^c = 3 \cdot (M_{z,g}^c)^2 \cdot \Sigma_{r,g}^c \tag{7b}$$

The multiplier factor 3 in Equation (7b) can ensure that the directional diffusion coefficients $D_{z,g}^c$ will be the same as the averaged diffusion coefficients D_g^c in isotropic materials.

III. GROUP-WISE TALLY FOR CMM

Based on the concept of cumulative migration area, as illustrated in Figure 2, cumulative-group quantities are necessary for calculating group-wise diffusion coefficients. But for

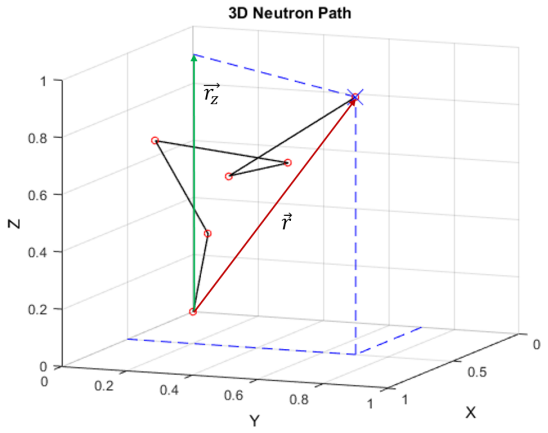

Fig. 3. Illustration of directional projection of cumulative migration vector.

the implementation in general Monte Carlo codes, it is not natural to tally cumulative-group quantities. In this paper, a new group-wise tally scheme is proposed to replace the previous way of directly tallying cumulative-group quantities in Monte Carlo codes.

According to Equation (5), cumulative-group migration area $(M_g^c)^2$ is defined as one sixth of the average of $(r_g)^2$, the square crow flight distance. The two positions related to r_g forms the cumulative migration vector $\boldsymbol{r}_g$, starting from the position where the neutron is born to the position where it is removed from cumulative group g. On the other hand, the "group-wise migration vector" can be represented by $\boldsymbol{l}_g$, starting from the position where the neutron's energy falls in group g to the position where it is removed from group g.

An illustration of the cumulative migration vectors and group-wise migration vectors is shown in Figure 4. On the left side of this figure, a neutron born at spatial point O (source origin) is depicted to undergo a series of scattering reactions and finally gets absorbed at point C. When this neutron is emitted (at the origin O), the neutron's energy belongs to group 1 in a given multi-group energy structure. As the neutron travels in the space, its energy varies as scattering reactions occur. In the scenario of the neutron in Figure 4, at point A, a down-scatter reaction slows down the neutron so that its energy after the reaction belongs to group 2. Similarly, at point B, the neutron's energy is changed from group 2 to group 3. Finally, after a few more scattering reactions (but the energy group is no longer changed), the neutron is absorbed at point C.

The right part in Figure 4 shows the "evolutionary history" of the neutron's energy versus the reaction sequence in time. For the purpose of illustration, the whole energy range is divided into 5 groups, with the darkest background color representing the group of the highest energy and the lightest color representing the group of lowest energy. The bright yellow line represents the neutron's energy corresponding to separate flights between each successive reactions as shown on the left part.

From the neutron's spatial and energetic variation record in Figure 4, for the first group, it is obvious that the cumulative-group migration vector and "group-wise migration vector" are the same, i.e., $\boldsymbol{r}_1 = \boldsymbol{l}_1 = \overrightarrow{OA}$.

For group 2 and group 3, the cumulative-group migration vector $\boldsymbol{r}_g$ can be decomposed into two components, as

$$\boldsymbol{r}_g = \boldsymbol{r}_{g-1} + \boldsymbol{l}_g \tag{8}$$

Thus for square crow flight distance, it's straightforward to employ vector math to obtain

$$(\boldsymbol{r}_g)^2 = (\boldsymbol{r}_{g-1})^2 + (\boldsymbol{l}_g)^2 + 2 \cdot \boldsymbol{r}_{g-1} \cdot \boldsymbol{l}_g \tag{9}$$

In this case the neutron's energy group variations happened in two consecutive groups, i.e., from group 1 to group 2 and from group 2 to group 3. More generally, if the neutron is in group gp (previous group) before a scattering reaction and group g afterwards, the geometrical relationships in Equation (8) and (9) will become

$$\boldsymbol{r}_g = \boldsymbol{r}_{gp} + \boldsymbol{l}_g \tag{10a}$$

$$(\boldsymbol{r}_g)^2 = (\boldsymbol{r}_{gp})^2 + (\boldsymbol{l}_g)^2 + 2 \cdot \boldsymbol{r}_{gp} \cdot \boldsymbol{l}_g \tag{10b}$$

The $(\boldsymbol{r}_g)^2$ and $(\boldsymbol{r}_{gp})^2$ in Equation (10b) are just the values used to compute the cumulative-group migration area $(M_g^c)^2$. In this way, starting from group 1, in which the cumulative group tally is the same as group-wise tally, $(\boldsymbol{r}_g)^2$ of all groups can be computed by a recursive process. In Equation (10b), the first term on the right hand side can be obtained recursively from previous groups. The second term and the third term can be computed using the information of the neutrons' positions, which can both be obtained through conventional group-wise tallies.

In this way, CMM can be implemented in a pure group-wise tally scheme and this removes the need for tallying cumulative-group tallies. The new group-wise tally scheme is equivalent to the cumulative-group tally but with higher efficiency. Additionally, the group-wise tally is more "natural" with conventional Monte Carlo tally systems.

1. Group-wise Tally Scheme

The new scheme using group-wise tallies is shown in the flowchart of Figure 5. The flowchart presents the tally scheme for one reaction of the tracked neutron. It is assumed that the neutron's energy group evolution history is (group gp) → (group g) → (group gn): before the reaction the neutron's energy is in group g, and after the reaction it's in group gn (new group). In addition, before the neutron enters group g, it was in group gp (previous group). Although the reaction only has a direct impact on group g and gn, the tally for this reaction will contribute to the migration area of group g. For instance, if this is a down-scatter case ($gn > g$), the neutron's energy has left cumulative group g, but not cumulative group gn. Thus the tally will need the information of group g and the previous group before it enters group g, i.e., group gp. For the special case of a neutron being born in group g (no previous group), the cumulative-group migration vector $\boldsymbol{r}_{gp}$ will be a zero vector thus the tally scheme is still general.

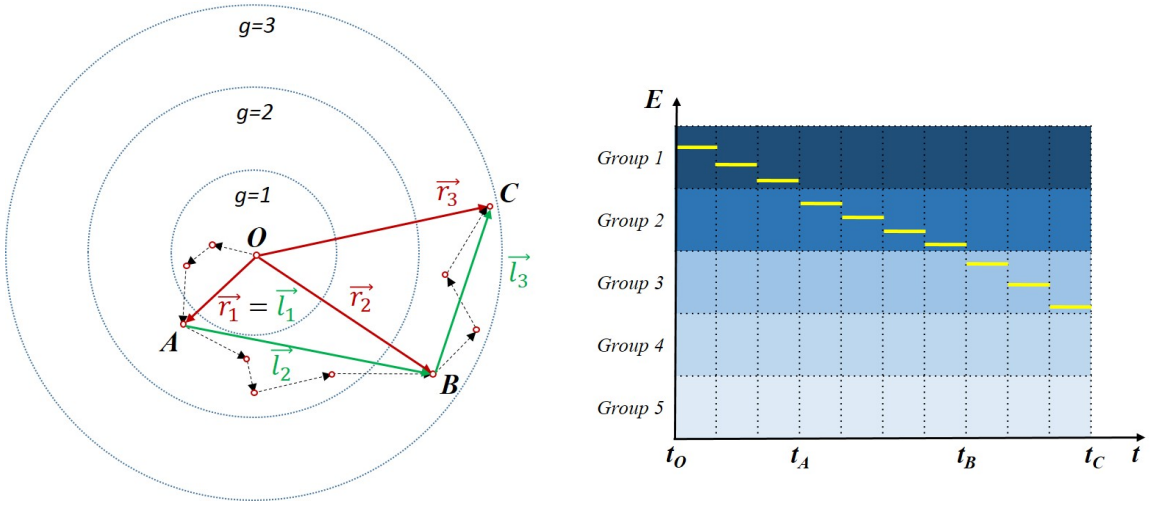

Fig. 4. Spatial and energetic illustration of an example of a neutron undergoing a series of scattering reactions and finally absorbed. *On the left*: flight tracks of the neutron (in black dashed line), cumulative-group migration vectors (in red) and group-wise migration vectors (in green); *On the right*: corresponding energy transitions during the neutron's traveling history (shown in yellow line).

In the flowchart, T_g is designated as the variable for storing the summation of all neutron's group-wise tallies in group g needed for computing cumulative migration area. For down-scatter and absorption reactions, only one tally in group g needs to be made. For up-scatter reactions, it will be more complicated to maintain the equivalence to cumulative migration area tallies, which will be further explained in following examples.

Using this group-wise tally scheme, all tallies needed for calculating migration area and diffusion coefficients are done group-wise. The spatial and energy information needed to complete the tallies are only related to group g (including group gp and gn). Compared with the cumulative-group tally scheme in the previous paper [6], the group-wise Monte Carlo tallies can entirely replace the cumulative ones and significantly simplifies implementation.

2. Calculation After Tallies

As in general Monte Carlo simulations, the statistical average of these tallied quantities can be computed after repeating the tally process for a large number of neutrons. As explained in the example neutron of Figure 4, for group 1, the cumulative-group migration vector and "group-wise migration vector" are the same, thus the average of $(\boldsymbol{r}_1)^2$ can be computed as

$$\langle(\boldsymbol{r}_1)^2\rangle = \frac{T_1}{N_1^C} \tag{11}$$

in which N_1^C is the net number of neutrons removed from cumulative group 1, which is just equal to the number of neutrons born in group 1.

For all subsequent groups, the average of $(\boldsymbol{r}_g)^2$ can be recursively computed as

$$\langle(\boldsymbol{r}_g)^2\rangle = \langle(\boldsymbol{r}_{g-1})^2\rangle \cdot \frac{N_{g-1}^C}{N_g^C} + \frac{T_g}{N_g^C} \tag{12}$$

in which N_g^C is the net number of neutrons removed from cumulative group g and it can be computed by accumulating the number of neutrons born in each group.

3. Tally Examples for Scatter Reactions

To better illustrate the scheme in Figure 5, the tally processes for two example neutrons are shown and explained in this section. Both neutrons have tracks similar to the one in Figure 4, but with different energy group transition histories. The energy group transition of the neutron in Figure 4 is (*group* 1) → (*group* 2) → (*group* 3), but for these two example neutrons they are (*group* 1) → (*group* 3) → (*group* 4) and (*group* 1) → (*group* 5) → (*group* 3), as shown in Figure 6. For simplicity, it's further assumed that both example neutrons have energy groups changed by scattering reactions at spatial points A and B, and are finally absorbed at C.

The first example neutron undergoes a series of pure down-scatter reactions, and the cumulative-group tally (as described in the previous paper on CMM [6]) and group-wise tally process are listed side-by-side in Table I. The only difference between this example neutron and the one in Figure 4 is that in the scenario of the neutron in Figure 4, the neutron's energy group variations both happened in two consecutive groups, while in Figure 6 the variations are not always in consecutive groups and can "jump over" groups (such as the transition of (group 1) → (group 3)).

As shown in the table, using the recursive relationship in Equation (12), group 2 gets the information tallied from group 1, which eliminates the redundancy in the cumulative-group tally. In addition, the recursive relationship actually enables all lower groups to "inherit" the information from group 1.

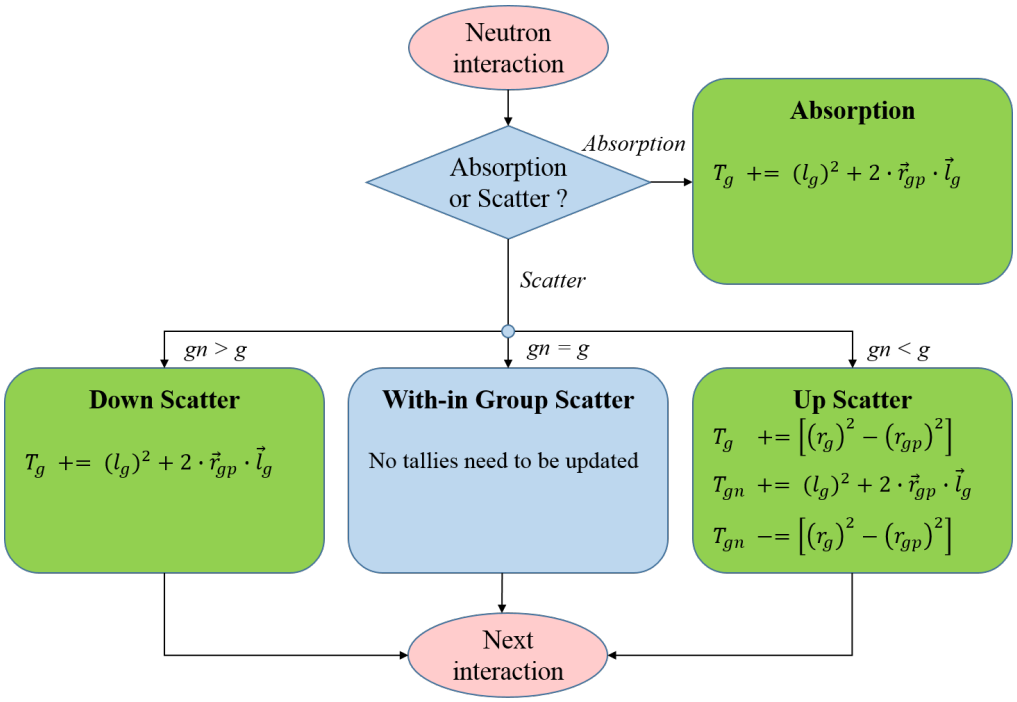

Fig. 5. Flowchart for the group-wise tally scheme using Cumulative Migration Method. It's assumed that the neutron's energy group evolution history is (group gp) → (group g) → (group gn). Before the reaction the neutron's energy is in group g, and after the reaction it's in group gn. In addition, before the neutron enters group g, it's in group gp.

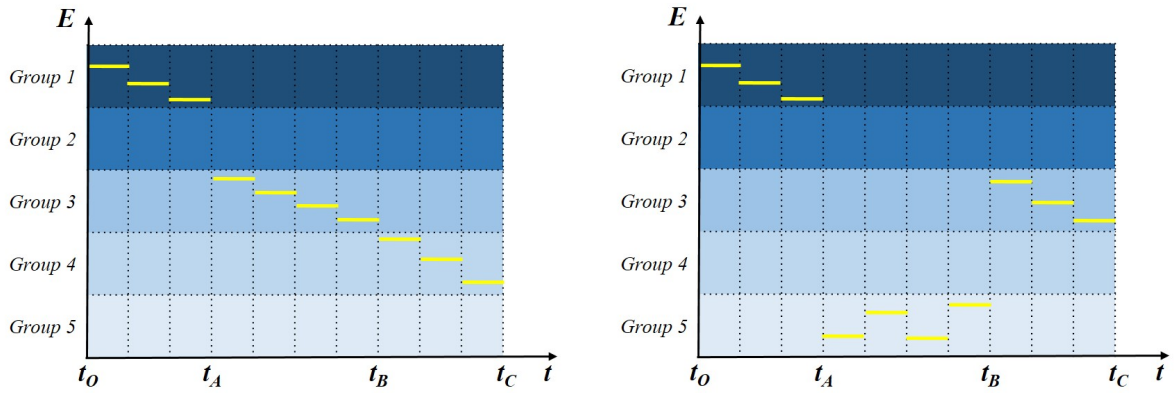

Fig. 6. The "evolutionary histories" of two example neutrons' energy versus reaction sequence. Both example neutrons have energy groups changed by scattering reactions at point A and B, and are finally absorbed at C. The energy group transitions are (*group* 1) → (*group* 3) → (*group* 4) and (*group* 1) → (*group* 5) → (*group* 3), respectively.

Thus at point A, there is a tally of $\overrightarrow{OA}^2$ recorded in group 3. Combined with the tally of $(\overrightarrow{AB}^2 + 2 \cdot \overrightarrow{OA} \cdot \overrightarrow{AB})$ at point B, it becomes $\overrightarrow{OA}^2 + (\overrightarrow{AB}^2 + 2 \cdot \overrightarrow{OA} \cdot \overrightarrow{AB}) = \overrightarrow{OB}^2$, which is the same as $(M_3^C)^2$ (the cumulative group tally in group 3) as shown on the left part of the table.

For the second example neutron, up-scatter reactions are shown in the rise of yellow line in the rightmost illustration in Figure 6. The cumulative-group and group-wise tally are also listed side-by-side in Table II.

As in the pure down-scatter case, the recursive relationship enables all lower groups to "inherit" tally information from higher groups, so all lower groups have implicitly recorded the tally of $\overrightarrow{OA}^2$ at point A, including group 5. Then for the up-scatter reaction, from which the neutron's energy is increased from group 5 to group 3, in addition to the tally of $(\overrightarrow{AB}^2 + 2 \cdot \overrightarrow{OA} \cdot \overrightarrow{AB})$ (as done for down-scatter reactions), another adjustment must be made to agree with the cumulative-group tally. As shown in the table, the dif-

TABLE I. The cumulative-group and group-wise tallies for the first example neutron, which undergoes a series of pure down-scatter reactions with the energy group transition history of (*group* 1) → (*group* 3) → (*group* 4). (The neutron's energy group is changed by scattering reactions which happened at point A and B, and it's finally absorbed at C.)

Group	Cumulative-group Tally				Group-wise Tally			
		at A	at B	at C		at A	at B	at C
1	$(M_1^C)^2$	$+\overrightarrow{OA}^2$			T_1	$+\overrightarrow{OA}^2$		
2	$(M_2^C)^2$	$+\overrightarrow{OA}^2$			T_2			
3	$(M_3^C)^2$		$+\overrightarrow{OB}^2$		T_3		$+\left(\overrightarrow{AB}^2 + 2\cdot\overrightarrow{OA}\cdot\overrightarrow{AB}\right)$	
4	$(M_4^C)^2$			$+\overrightarrow{OC}^2$	T_4			$+\left(\overrightarrow{BC}^2 + 2\cdot\overrightarrow{OB}\cdot\overrightarrow{BC}\right)$
5	$(M_5^C)^2$			$+\overrightarrow{OC}^2$	T_5			

ference of $\overrightarrow{OB}^2$ and $\overrightarrow{OA}^2$ must be added to group 5 and subtracted from group 3. It makes more sense when incorporating the absorption reaction at point C, which has a total tally of $(\overrightarrow{OA}^2 - \overrightarrow{OB}^2 + \overrightarrow{OC}^2)$ for group 3 in cumulative-group tally. In group-wise tally for group 3, the "inherited" tally from group 1, $\overrightarrow{OA}^2$, is finally converted into $\overrightarrow{OC}^2$) by the geometrical relations: $\overrightarrow{OA}^2 + (\overrightarrow{AB}^2 + 2\cdot\overrightarrow{OA}\cdot\overrightarrow{AB}) + (\overrightarrow{BC}^2 + 2\cdot\overrightarrow{OB}\cdot\overrightarrow{BC}) = \overrightarrow{OC}^2$. So the subtracted term of $(\overrightarrow{OB}^2 - \overrightarrow{OA}^2)$ balances the non-geometrical but physical tallies in the cumulative-group tally.

The group-wise tally scheme for CMM has been implemented and tested in a prototype Monte Carlo code. As explained in this section, it is mathematically equivalent to the cumulative-group tally, thus duplication of results is omitted.

IV. RESULTS AND ANALYSIS

A 3D Monte Carlo simulation is carried out using OpenMC for a simplified model of the TREAT fuel assembly. In the 3D model, on the horizontal plane (x and y directions) reflective boundary conditions are employed, and axially (z direction) it consists of the top reflector of 64 cm, the fuel region of 120 cm and bottom reflector of 60 cm, as shown in Figure 7. Vacuum boundary conditions are employed outside of the top and bottom reflectors in the axial direction.

In addition, the eigenvalue as well as flux distribution for the same problem are computed by a 1D 11-group homogenized diffusion calculation. The 11-group diffusion coefficients and cross sections are tallied and computed using OpenMC for the fuel and reflector separately, each with the actual configuration in 2D horizontal plane and infinite in axial direction, as traditionally done for PWR fuel assemblies. Using the 3D Monte Carlo results as a reference, it is compared with the 1D 11-group diffusion results with diffusion coefficients generated by four different approaches. The four approaches include:

- D_g^{os} : Out-scatter approximation for computing $\Sigma_{tr,g}^{os}$, then $D_g^{os} = 1/3\Sigma_{tr,g}^{os}$.
- D_g^{as} : Asymptotic out-scatter approximation for computing $\Sigma_{tr,g}^{as}$, then $D_g^{as} = 1/3\Sigma_{tr,g}^{as}$.
- D_g^{CMM} : CMM method for tallying cumulative migration area $(M_g^c)^2$ using OpenMC, then computing D_g^c and D_g.

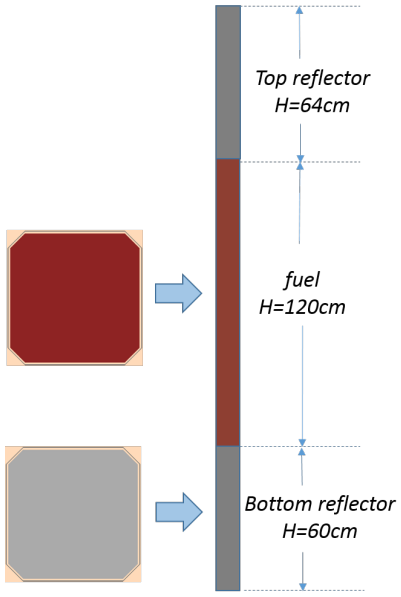

Fig. 7. The axial layout of the simplified TREAT fuel assembly model.

- $D_{z,g}^{CMM}$: CMM method for tallying directional cumulative migration area $(M_{z,g}^c)^2$ using OpenMC, then computing $D_{z,g}^c$ and $D_{z,g}$.

The results of the eigenvalue for this problem are listed and compared in Table III. Compared to the 3D OpenMC results, k_{eff} from the diffusion calculation with diffusion coefficients from CMM produce much more accurate results than those from out-scatter approximations. The accuracy of flux distribution is also improved with CMM by reducing the max relative error of roughly 6% with out-scatter approximations to about 2% with CMM. The accuracy of group-wise flux distribution is improved in both the fuel region and the reflector region.

Comparison of the 11-group diffusion coefficients computed by different methods is shown in Table IV with the energy group structure. It is obvious that the diffusion coefficients of group 1 and group 2 generated by CMM are larger

TABLE II. The cumulative-group and group-wise tallies for the second example neutron, which undergoes a series of both down-scatter and up-scatter reactions with the energy group transition history of (*group* 1) → (*group* 5) → (*group* 3). (The neutron's energy group is changed by scattering reactions which happened at point A and B, and it's finally absorbed at C.)

		Cumulative-group Tally				Group-wise Tally		
Group		at A	at B	at C		at A	at B	at C
1	$(M_1^C)^2$	$+\overrightarrow{OA}^2$			T_1	$+\overrightarrow{OA}^2$		
2	$(M_2^C)^2$	$+\overrightarrow{OA}^2$			T_2			
3	$(M_3^C)^2$	$+\overrightarrow{OA}^2$	$-\overrightarrow{OB}^2$	$+\overrightarrow{OC}^2$	T_3		$+\left(\overrightarrow{AB}^2 + 2\cdot\overrightarrow{OA}\cdot\overrightarrow{AB}\right) - \left(\overrightarrow{OB}^2 - \overrightarrow{OA}^2\right)$	$+\left(\overrightarrow{BC}^2 + 2\cdot\overrightarrow{OB}\cdot\overrightarrow{BC}\right)$
4	$(M_4^C)^2$	$+\overrightarrow{OA}^2$	$-\overrightarrow{OB}^2$	$+\overrightarrow{OC}^2$	T_4			
5	$(M_5^C)^2$			$+\overrightarrow{OC}^2$	T_5		$+\left(\overrightarrow{OB}^2 - \overrightarrow{OA}^2\right)$	

TABLE III. Comparison of eigenvalues computed by different approahes for the TREAT fuel assembly problem.

Method	k_{eff}	Difference
OpenMC	1.44399 (±0.00006)	(reference)
Diffusion by D_g^{os}	1.45750	0.01351
Diffusion by D_g^{as}	1.45680	0.01281
Diffusion by D_g^{CMM}	1.44738	0.00339
Diffusion by $D_{z,g}^{CMM}$	1.44413	0.00014

than those of the out-scatter approximation, which impact the axial leakage. CMM improves the accuracy of the diffusion coefficients by better representing the anisotropic neutron transport of the problem.

TABLE IV. Comparison of 11-group diffusion coefficients computed by different methods. (The units of diffusion coefficients in this table are all *cm*.)

Group & Energy (MeV)		D_g^{os}	D_g^{as}	D_g^{CMM}	$D_{z,g}^{CMM}$
1	(3.329E00-2.000E+1)	3.055	2.678	4.068	4.081
2	(1.156E-1-3.329E00)	1.531	1.498	1.748	1.773
3	(3.481E-3-1.156E-1)	0.969	1.008	1.010	1.039
4	(1.327E-4-3.481E-3)	0.944	0.993	0.991	1.020
5	(8.100E-6-1.327E-4)	0.942	0.990	0.987	1.014
6	(6.250E-7-8.100E-6)	0.942	0.989	0.985	1.011
7	(2.096E-7-6.250E-7)	0.927	0.983	0.970	0.997
8	(7.650E-8-2.096E-7)	0.906	0.973	0.951	0.980
9	(4.730E-8-7.650E-8)	0.877	0.956	0.923	0.951
10	(2.001E-8-4.730E-8)	0.836	0.928	0.879	0.908
11	(0.000E00-2.001E-8)	0.697	0.814	0.749	0.777

V. CONCLUSIONS

The Cumulative Migration Method (CMM) overcomes shortcomings in various approximation methods for computing multi-group diffusion coefficients and transport cross sections. Based on the theory of cumulative migration area and its relationship with diffusion coefficients, CMM is further developed to compute directional diffusion coefficients in a natural approach. The 11-group diffusion calculations for a simplified TREAT fuel assembly model showed that the results for both eigenvalue and flux distribution can be more accurate using the directional diffusion coefficients computed by CMM.

The new group-wise tally is equivalent to cumulative-group tally and it produces identical results, with the added benefit of simplifying the tally edits needed in the previous cumulative-group implementation for Monte Carlo codes.

Moreover, the new group-wise tally method for cumulative migration area is also a promising bridge to computing heterogeneous diffusion coefficients and transport cross sections.

VI. ACKNOWLEDGMENTS

This research is being performed using funding received from the DOE Office of Nuclear Energy's Nuclear Energy University Programs (contract number: DE-NE0008578). This work is also partially funded by the Idaho National Laboratory under Contract No. DE-AC07- 05ID14517 with the US Department of Energy.

REFERENCES

1. T. NEWTON and J. HUTTON, "The next generation WIMS lattice code: WIMS9," *Proceedings of New Frontiers of Nuclear Technology, PHYSOR*, pp. 7–10 (2002).
2. H. HURIA, Y. CHAO, M. KICHTY, T. DOWNS, Y. SHATILLA, T. MORITA, and F. ADORJAN, "Theory and methodology of Westinghouse PHOENIX-H/ANC-H for hexagonal PWR cores," *Transactions of the American Nuclear Society*, **71**, *CONF-941102*– (1994).
3. G. MARLEAU, R. ROY, and A. HÉBERT, "DRAGON: a collision probability transport code for cell and supercell calculations," *Report IGE-157, Institut de génie nucléaire, École Polytechnique de Montréal, Montréal, Québec* (1994).
4. E. A. VILLARINO, R. J. STAMM'LER, A. A. FERRI, and J. J. CASAL, "HELIOS: angularly dependent col-

lision probabilities," *Nuclear Science and Engineering*, **112**, *1*, 16–31 (1992).
5. G. POMRANING, "Flux-limited diffusion theory with anisotropic scattering," *Nuclear Science and Engineering*, **86**, *4*, 335–343 (1984).
6. Z. LIU, K. SMITH, and B. FORGET, "A Cumulative Migration Method for Computing Rigorous Transport Cross Sections and Diffusion Coefficients for LWR Lattices with Monte Carlo," PHYSOR (2016).
7. B. R. HERMAN, B. FORGET, K. SMITH, and B. N. AVILES, "Improved diffusion coefficients generated from Monte Carlo codes," Tech. rep., American Nuclear Society, 555 North Kensington Avenue, La Grange Park, IL 60526 (United States) (2013).
8. P. K. ROMANO and B. FORGET, "The OpenMC Monte Carlo particle transport code," *Annals of Nuclear Energy*, **51**, 274–281 (2013).
9. N. HORELIK, B. HERMAN, B. FORGET, and K. SMITH, "Benchmark for evaluation and validation of reactor simulations (BEAVRS)," Tech. rep., American Nuclear Society, 555 North Kensington Avenue, La Grange Park, IL 60526 (United States) (2013).
10. K. SMITH, "Nodal Diffusion Methods: Understanding numerous unpublished details," PHYSOR (2016).
11. J. D. BESS and M. D. DEHART, "Baseline Assessment of TREAT for Modeling and Analysis Needs," Tech. rep., Idaho National Laboratory (INL), Idaho Falls, ID (United States) (2015).